ECS Transactions, 16 (49) 141-149 (2009)
10.1149/1.3159318 ©The Electrochemical Society

Nonaqueous Solvatochromic Behavior of Nile Blue A Perchlorate in Imidazolium – Exchanged Clays and its Implication Toward Exfoliation in Polymeric Composites*

D. M. Fox[a], P. C. Trulove[b], H. C. De Long[c], J. W. Gilman[d], and P. H. Maupin[e]

[a] Department of Chemistry, American University, Washington, District of Columbia 22016, USA
[b] Department of Chemistry, U.S. Naval Academy, Annapolis, Maryland 21402, USA
[c] Directorate of Math, Info, & Life Sciences, U.S. Air Force Office of Scientific Research, Arlington, Virginia 22203, USA
[d] Fire Research Div., Building & Fire Research Laboratory, National Institute of Standards & Technology, Gaithersburg, MD 20899, USA
[e] Division of Chemical Sciences, Geosciences, and Biosciences, Office of Basic Energy Sciences, U.S. Department of Energy, Washington, District of Columbia 20585, USA

Ultraviolet (UV) and visible (VIS) light absorption and emission spectroscopy is a powerful tool for probing solute-solvent interactions. Recently, we have identified the use of Nile Blue as a sensitive fluorescent probe in identifying the local nanoenvironment, such as confinement within clay nanolayers. In this study we examine the solvatochromic behavior of Nile Blue adsorbed montmorillonite in solvents of varying polarity and the influence of an adsorbed imidazolium surfactant. The fluorescence behavior in solvents is compared to its behavior in polymers with similar chemical structures to the solvents.

Introduction

Electronic emission and absorption spectroscopy can provide information regarding dye orientation at the clay surface, the interaction between the π – system of the dye and the oxygen lone pair of the clay surface, the dye aggregation at the clay surface, the polarity of the solvent, and the confinement of dye in the clay galleries (1,2). In this study, we measure the absorbance and fluorescence of montmorillonite exchanged with Nile Blue (5 % or 10 % cation exchange capacity, CEC). The solvochromatic effects were compared to Nile Blue exchanged clays with co-exchanged 1,2-dimethyl-3-hexadecylimidazolium cations (remainder of CEC) as well as Nile Blue perchlorate (no clay) in solution. A variety of nonaqueous solvents were chosen to cover a range of polarity and hydrogen bonding ability. Both absorption and emission peaks are assigned to specific species and interactions to elucidate the effects of local polarity and nanoconfinement on the spectral properties of Nile Blue.

Recently, we identified the use of Nile Blue as a fluorescent probe in identifying the level of exfoliation of clay layers in polymer – layered silicate nanocomposites (3). Toluene and N,N-dimethylformamide were chosen among the solvents, because they mimic the chemical structures of the repeating monomeric units of the common

* Official contribution of the National Institute of Standards and Technology, and not subject to copyright in the United States.

commodity plastics, polystyrene and polyamides. Correlations between the emission spectra of the solutions and polymer nanocomposites are discussed.

The abbreviations used throughout this manuscript are shown in Table I.

TABLE I. Frequently Used Abbreviations in this Manuscript

Abbreviation Used	Compound Name
NB	Nile Blue A cation
NBB	De-protonated Nile Blue cation
MT	Montmorillonite
CEC	Cation exchange capacity
DMHdI	1-Hexadecyl-2,3-dimethylimidazolium cation
DMF	N,N-Dimethylformamide
DMSO	Dimethylsulfoxide
EtAc	Ethyl acetate
EtLac	Ethyl L-lactate
PS	Polystyrene
PA	Polyamide (Nylon)

Experimental

Materials

All solvents (Sigma), Nile Blue A perchlorate (NB-ClO_4, Sigma), and sodium montmorillonite (Na-MT, Southern Clay Products) were used as received. Exchanged clays containing 5 % or 10 % CEC of the Na-MT (both with and without surfactant) and polymer nanocomposites containing 5 % by mass exchanged clay using a melt blending technique, were prepared as described previously (3). The 1-hexadecyl-2,3-dimethylimidazolium cation (DMHdI) was used as the surfactant.

Spectral Techniques

3 mg of clay was added to 10 mL of solvent, and the absorption spectra was measured after 1 min, 1 hr, 1 d, and 1 wk using an OceanOptics 2000 UV/VIS spectrometer. 14 x 10^{-6} mol/L NB solutions were prepared to match the amount of nile blue in 5 % CEC MT samples. Fluorescence measurements were taken after 1 min, 1 hr, and 1 wk using an OceanOptics USB2000 spectrometer adapted for fiber optic input with a 100 μm entrance slit width and a 365 nm, 300 W black light excitation source. Mass measurements have an uncertainty of $2\sigma = \pm 0.4$ mg, volume measurements have an uncertainty of $2\sigma = \pm 0.2$ mL and wavelengths have an uncertainty of $2\sigma = \pm 0.22$ nm.

Results and Discussion

To investigate the solvatochromic behavior of NB-ClO_4, NB exchanged MT, and NB/DMHdI co-exchanged MT, along with chromism of dye-exchanged clay / polymer nanocomposites, we investigated the absorption and emission spectra of systems containing the Nile Blue A cation.

Solvatochromic Absorance of NB and NB-MT

The visible absorbance spectra of Nile Blue A perchlorate in 7 nonaqueous solvents is shown in Figure 1. The peak between 620 nm and 640 nm is assigned to the NB monomer and the shoulder around 590 nm is assigned to the $(NB)_2$ dimer (4). Douhal has shown that the peak between 505 nm and 520 nm is due to deprotonation of monomers (NBB) to electron donating solvents (5). Similar to his study, we found that both the NB and NBB peaks exhibit slight shifts that correlate to the solvent polarizability parameter (π^*). Nile Blue A perchlorate was not soluble in toluene.

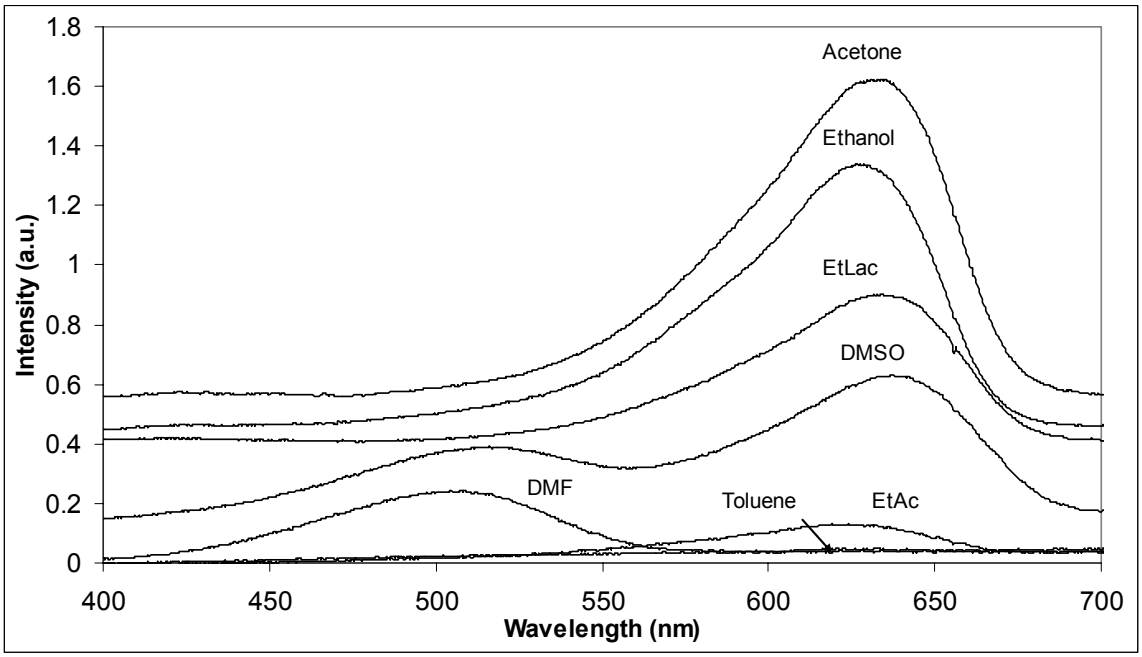

Figure 1. Visible absorbance spectra of 14 μM NB in nonaqueous solvents. Plots have been shifted upwards for clarity and intensity is in arbitrary units (a.u.).

The absorbance spectra of dye-exchanged clay (10 %NB-MT) in these same solvents is shown in Figure 2. No absorption was detected in toluene, ethanol, ethyl acetate, and ethyl L-lactate. MT has a low degree of swelling or forms precipitates in these solvents (6,7), and the presence of NB does not expand the layers enough to facilitate appreciable solvent – dye interactions. In acetone, a large red shift was observed and in DMSO, the NBB peak intensified at the expense of a total loss in the NB peak. The red shift has been attributed to the polarization of the dye when its π system interacts with oxygen lone pairs of electrons on the clay surface (1,8). The size (and direction) of the shift accompanying adsorption onto clay is affected by aggregate concentration of the dye prior to adsorption (8), the surface charge density of the clay (8-10), the ability of the π system to approach the clay surface, (1) the chemical properties of the dye (11), and the presence of a surfactant (12). In our system, MT has a highly charged surface and NB is polarizable with a semi-labile proton. Thus, the results here suggest a proton transfer to the clay surface and nonionic NBB adsorption, rather than just polarization. As shown in Figure 2b, the adsorption of NBB onto MT in DMF results in a modest increase in intensity without any wavelength shift.

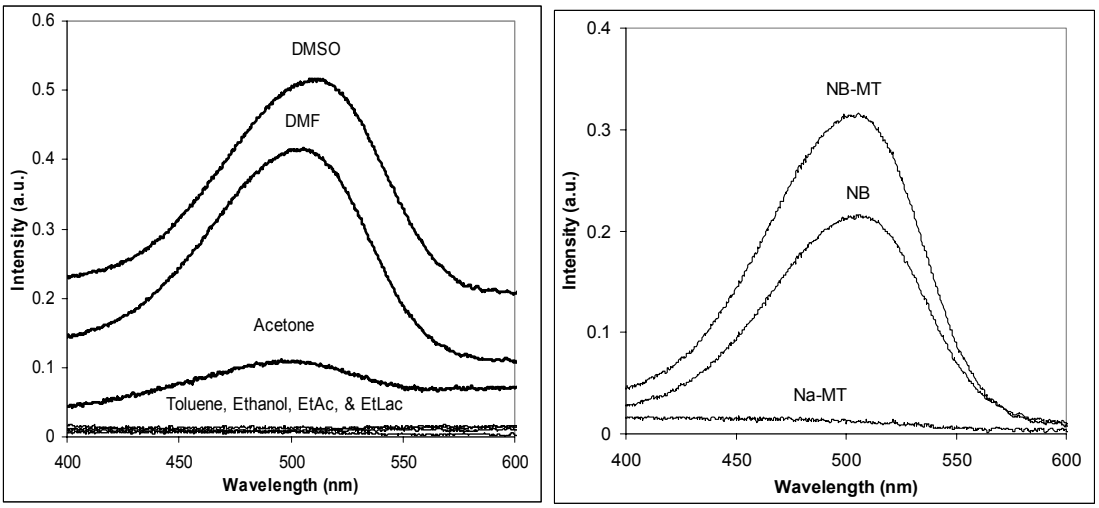

Figure 2. (a) Visible absorbance spectra of 10 %NB-MT in nonaqueous solvents. Plots have been shifted upwards for clarity. (b) Comparison of Na-MT, NB, and 5 %NB-MT absorbance spectra in DMF.

The presence of surfactant within the clay layers significantly alters the absorption spectra of NB-MT, as shown in Figure 3a. The most notable effects are that NB absorbs visible light in all solvents in the presence of DMHdI, (illustrating the surfactant ability of this imidazolium cation) and the complete loss in NB peak in the 625 nm to 635 nm region. The peak absorbance varies between 504 nm and 535 nm, and is roughly correlated to the polarizability (π^*) and hydrogen bonding acceptor (β) solvent parameters, as illustrated in Figure 3b. The plots are red shifted ($\approx$ 15 nm) from 5 %NB-MT due to the decreased polarity near the clay surface. Breen and Loughlins also noted a red shift in methylene blue adsorbed MT (12). They attributed this shift to hemimicelle solubilization of the dye leading to increased monomers, increased distance between the dye and clay surface, and reduced dye polarization. It is possible that the long alkyl chains of the DMHdI surfactant create a favorable environment for NBB solvation and promotes the proton transfer to the clay surface exchange sites. The relative absorbance peak positions in ethanol and EtLac exhibited a larger red shift than would be expected based on their π^* or β values. This larger shift has been attributed to hydrogen bonding interactions between NB and hydrogen donating solvents (5,13). Ethanol and EtLac are the only solvents in this study with appreciable hydrogen bonding donating parameter (α) values, corroborating their assignments.

Solvatochromic Emission of NB-MT

Nile Blue is most widely used as a fluorescent probe. At higher concentrations, NB is known to form aggregates, which reduces quantum yield (14). To minimize aggregate formation and quenching, emission spectra of only the 5 % CEC exchanged NB samples were measured. An emission comparison of 5 %NB-MT to (5%NB+95%DMHdI)-MT in DMF and toluene is shown in Figure 4. Emission spectra of 14 μmol/L NB and the NB exchanged clays in all seven solvents were also examined (not shown), but their analysis is beyond the scope of this study.

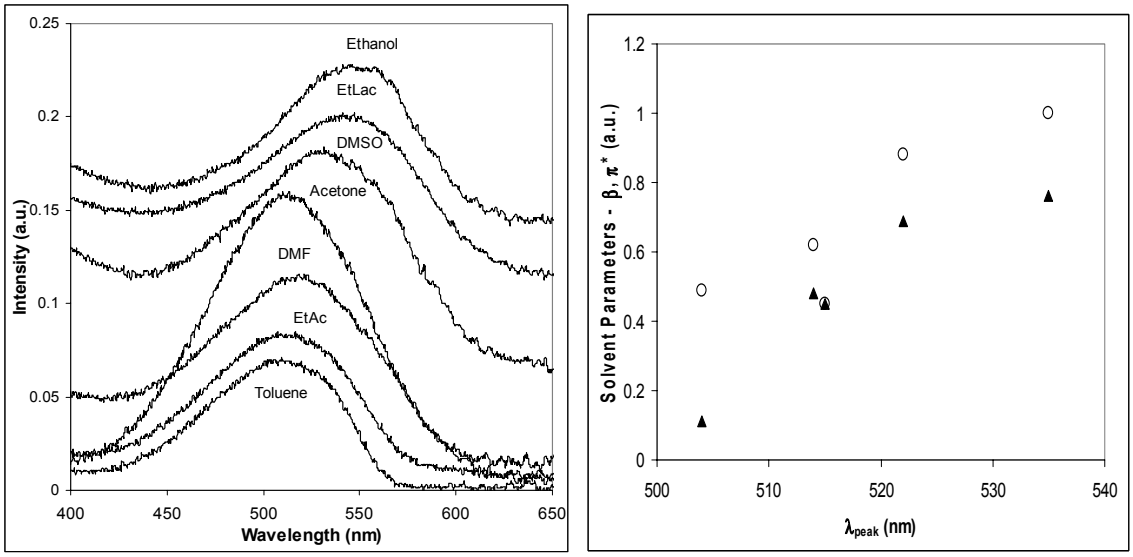

Figure 3. (a) Visible absorbance spectra of (10%NB+90%DMHdI)-MT in nonaqueous solvents. Plots have been shifted upwards for clarity. (b) Polarizability (π*,▲) and hydrogen bonding acceptor (β,○) solvent parameters vs peak absorbance of (10%NB+90%DMHdI)-MT in toluene (504 nm), acetone (514 nm), EtAc (515 nm), DMF (522 nm), and DMSO (535 nm).

Excitation of 5 %NB-MT in DMF leads to a strong emission band at 730 nm overlapping smaller bands at 760 nm. (cf Figure 4a) Excitation of (5%NB+95%DMHdI)-MT produces a smaller Stokes shift of the main band (615 nm) and the apparent loss of the shoulders. The Stokes shift is significantly greater than the absorption red-shift observed for the imidazolium exchanged clays, suggesting that it is not due purely to polarity differences. Douhal noted the presence of two emission bands (578 nm and 685 nm) for NB in dimethylaniline (DMA), which he assigned to the proton transferred dye – solvent pair (NBB – $DMAH^+$) formed from excitation of NBB-$DMAH^+$, followed by either relaxation (578 nm) or excited state proton transfer and relaxation from the re-protonated NB excited state (685 nm) (5). Excited state relaxation in DMF favors the latter for 5%NB-MT, while the presence of DMHdI hinders or slows this excited state proton transfer, resulting in relaxation without excited state proton transfer.

Excitation of these clays in toluene exhibits significantly different emission spectra than in DMF. 5 %NB-MT is not soluble in toluene, so it does not exhibit any fluorescence. Excitation of (5%NB+95%DMHdI)-MT produces a smaller Stokes shift than in DMF, with strong emission bands at 485 nm and 565 nm. (cf Figure 4b) The presence of a NBB emission (565 nm) and lack of a NB emission supports the earlier hypothesis that DMHdI helps facilitate proton transfer from NB to the clay surface in all solvents studied. Studies on the nanoconfinement of NB in porous nonpolar sol-gels reveal that blue shifts are observed when the nanoconfinement is less than 7.5 nm, and the blue shifts become larger as the solvent medium polarity is lowered (15, 16). The height of the MT layers is between 1 nm and 4 nm, depending on the cation exchanged. Therefore, 40 nm blue shift of this peak may be due to the emission NBB in a solvent intercalated clay structure. The emission band at 485 nm is less clear, though smaller Stokes shifts have been reported for various charge transfer and aggregated forms of Nile Blue and similarly structured dyes in low polarity solvents (5, 16).

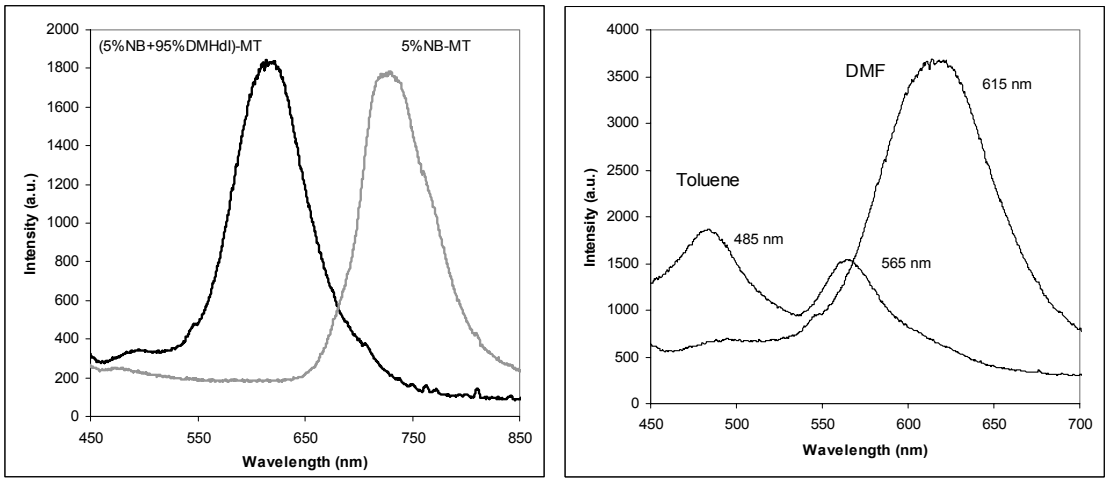

Figure 4. (a) Emission spectra of 5%NB-MT and (5%NB+95%DMHdI)-MT in DMF and (b) (5%NB+95%DMHdI)-MT in DMF and toluene using a black light excitation source (365 nm).

Emission of NB-MT / Polymer Nanocomposites

The emission spectra of (5%NB+95%DMHdI)-MT in polyamides (PA) and polystyrene (PS) exhibit nearly identical features to the emission spectra in DMF and toluene, respectively. (cf Figure 5) PA-6 nanocomposites prepared with 5 %NB-MT exhibits broad emission spectra with small Stokes shifts (not shown) and distinctive, but weak peaks at 498 nm, 608 nm, and 672 nm. The low intensity of these peaks suggests that there are a large number of NB aggregates and minimal dye – polymer interactions. Nanocomposites prepared from (5%NB+95%DMHdI)-MT exhibit emission bands that depend on the extrusion time. After 1 minute, a peak arises at 565 nm and after 7 min, this peak disappears in favor of additional peaks at 605 nm and 695 nm. These exhibit slight Stokes shifts relative to DMF (15 nm to 20 nm), but have nearly identical shapes.

TEM images of these composites (cf Figure 6) reveal that Na-MT produces intercalated structures and large tactoids while DMHdI-MT produces mainly intercalated structures after 1 minute (not shown) and nearly fully exfoliated structures after 7 minutes (Figure 6b) of melt-blending with PA-6. Use of 5 % NB in these clays (not pictured) does not alter the intercalation/exfoliation structures of the clay. The emission at 565 nm has been assigned to intercalated structures while the peak at 605 nm has been assigned to fluorescence of exfoliated clay structures in the polymer matrix (3). The peak at 498 nm has not been previously assigned, though it may be due to the internal electron transfer of the excited state Nile Blue, as discussed previously.

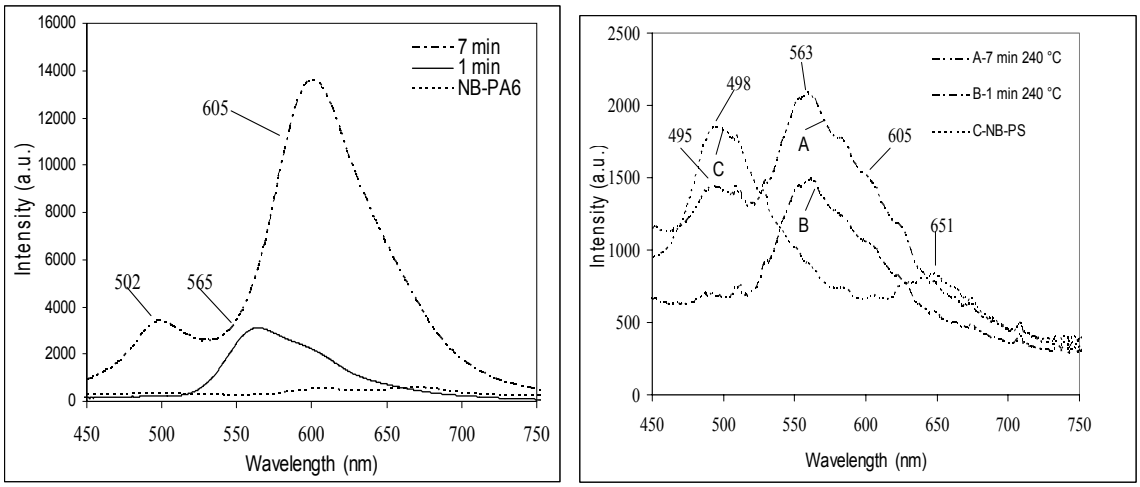

Figure 5. (a) Emission spectra of PA-6 clay nanocomposite with 5 % by mass 5 %NB-MT and (5%NB+95%DMHdI)-MT using a black light excitation source (365 nm). (b) Emission spectra of PS clay nanocomposite with 5 % by mass (5%NB+95%DMHdI)-MT using a 407 nm excitation source.

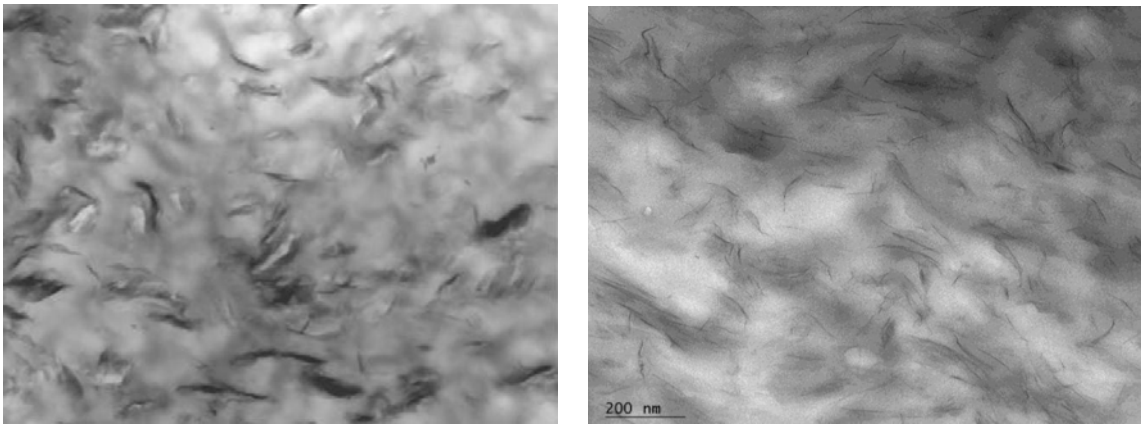

Figure 6. TEM images of PA-6 clay nanocomposite (a) with 5 % by mass Na-MT and (b) with 5 % by mass DMHdI-MT.

Comparison of toluene with PS (Figure 5b) also illustrates nearly identical emission spectra. The PS composites begin with a single emission peak at 565 nm and a small shoulder at 605 nm. Extensive shear mixing produces an additional small peak at 498 nm and slight increase in fluorescence intensities, but does not otherwise change. TEM and XRD analyses (not shown) indicate that these composites exhibit limited exfoliation with clays structures that are dominated by small intercalated tactoids. The emission at 565 nm has been assigned to fluorescence of intercalated clay structures in the polymer matrix (3). These peak assignments are nearly identical to the peaks observed in the solvents with similar chemical structures, and the solvent studies confirm that Nile Blue can be used as a fluorescent probe to identify the local polarity and local nanostructure, such as nanoconfinement. The correlation of polymer to solvent emission spectra indicate that dye absorbed clay solutions can be used to predict polymer – clay structure, providing a quick and potentially automated method for screening polymers, clays, and surfactants in the quest for improving dispersion and exfoliation in hydrophobic polymers.

Conclusions

This study examines the ability of Nile Blue A perchlorate to probe the local nanostructure of solvents and similarly structured polymers. The ability of the NB cation to deprotonate strongly affects both its absorbance and emission behavior. The presence of DMHdI was found to have profound affects on the solvatochromic behavior of NB adsorbed montmorillonite. Not only does this surfactant improve the solubility of the exchanged clays in all solvents studied, but it also stabilizes the deprotonated nile blue cation and reduces the number of UV/VIS absorbing and fluorescing species. The complex photoproperties of NB makes it a sensitive probe of the local nanoenvironment. The emergence of a second fluorescence peak when imidazolium compound is added to clay layer supports behavior attributed to nanoconfinement of the dye. Due to similarities between solvent and polymer fluorescence spectra, MT exfoliation may be probed by fluorescence in solvents with similar structure. This provides an opportunity to develop fast and automated tests for optimizing nanodispersion and exfoliation of clay in polymer systems.

Acknowledgments

The policy of the National Institute of Standards and Technology (NIST) is to use metric units of measurement in all its publications, and to provide statements of uncertainty for all original measurements. In this document however, data from organizations outside NIST are shown, which may include measurements in non-metric units or measurements without uncertainty statements. The identification of any commercial product or trade name does not imply endorsement or recommendation by NIST, the U.S. Air Force (USAF), U.S. Navy (USN), or U.S. Department of Energy (DOE). Opinions, interpretations, conclusions, and recommendations are those of the authors and are not necessarily endorsed by NIST, USAF, USN, or DOE.

References

1. M. J. Tapia Estevez, F. Lopez Arbeloa, T. Lopez Arbeloa, and I. Lopez Arbeloa, *Langmuir*, **9**, 3629, (1993).
2. G. B. Dutt, S. Doraiswamy, and N. Periasamy, *J. Chem. Phys.*, **94**, 5360, (1991).
3. P. H. Maupin, J. W. Gilman, R. H. Harris Jr., S. Bellayer, A. J. Bur, S. C. Roth, M. Murariu, A. B. Morgan, and J. D. Harris, *Macromol. Rapid Commun.*, **25**, 788, (2004).
4. C. Nasr and S. Hotchandani, *Chem. Mater.*, **12**, 1259, (2000).
5. A. Douhal, *J. Phys. Chem.*, **98**, 13131, (1994).
6. E. R. Graber and U. Mingelgrin, *Environ. Sci. Technol.*, **28**, 2360, (1994).
7. D. L. Ho and C. J. Glinka, *Chem. Mater.*, **15**, 1309, (2003).
8. Z. Klika, P. Capkova, P. Horakova, M. Valaskova, P. Maly, R. Machan, and M. Pospisil, *J. Colloid Interf. Sci.*, **311**, 14, (2007).
9. S. Yariv, in *Organo-Clay Complexes and Interactions*, S. Yariv and H. Cross, Editors, p. 463, Marcel Dekker, New York, (2002).
10. J. Buydk and P. Komadel, *J. Phys. Chem. B*, **101**, 9065, (1997)
11. J. Bujdak and N. Iyi, *J. Phys. Chem. B*, **110**, 2180, (2006).
12. C. Breen and H. Loughlin, *Clay Miner.*, **29**, 775, (1994).
13. D. I. Kreller and P. V. Kamat, *J. Phys. Chem.*, **95**, 4406, (1991).

14. J. Jose, Y. Yueno, and K. Burgess, *Chem. Eur. J.*, **15**, 418, (2009).
15. R. Baumann, C. Ferrante, F.W. Deeg, C. Brauchle, *J. Chem. Phys.*, **114**, 5781 (2001).
16. M. Krihak, M. T. Murtagh, M. R. Shahriari, *J. Sol Gel Technol.*, **10**, 153, (1997).